PHY293 Weight 2 Lab

Investigating Wavelengths, Index of Refraction and Coefficients of Thermal Expansion Using a Michelson Interferometer

November 11, 2025

Aarya Shah 1010871157 | Sara Parvaresh Rizi 1010913451

Abstract

This experiment used a Michelson interferometer to investigate the wavelength of green light, the index of refraction of a cube, and the thermal expansion of aluminum. The Michelson interferometer formulas for wavelength, index of refraction, and coefficient of thermal expansion all agreed with the data, with all measured values within 2% of theoretical predictions. The wavelength of green light was determined as (497±5) nm, the index of refraction of the cube as 1.50±0.01, and the thermal expansion of Al had (2.28 x 10^{-5} ± 3.21 x 10^{-13}) 1/K.

1. Intro

Interferometers are important devices used in the study of interference patterns, used to measure differences in distances with precision better than a micron (micrometre). They are divided into two main classes: division of wavefront and division of amplitude. This lab used a Michelson interferometer, which employs a division of amplitude scheme [1].

The wavelength of green light was calibrated using Equation (1), where λ corresponds to the wavelength, N is the number of fringes that appear or disappear, and Δx is the distance moved by the mirror.

$$N\lambda = 2\Delta x \quad (1)$$

The index of refraction (n) based on wavelength of light (λ) and angle moved (Θ) can be approximated to a quadratic equation for small angles, as shown in Equation (2).

$$N \simeq \frac{t}{\lambda}\Theta^2\left(1 - \frac{1}{n}\right) \quad (2)$$

The thermal expansion of aluminum, α, can be approximately linear, as shown in Equation (3), where N is the number of fringes counted, λ the wavelength, L_0 the initial length of the aluminum, and ΔT the temperature difference from the base temperature.

$$N \approx \frac{2L_0}{\lambda}\alpha\Delta T \quad (3)$$

In this lab, we measure the wavelength of the green laser and the red LED, the index of refraction of a plastic square prism, and the thermal expansion coefficient of aluminum.

2. Materials and Methods

The methods in this lab report adhere to the outlines in the 'Interferometry' manual [1]**.** Figure 1 displays and labels the equipment used in the lab.

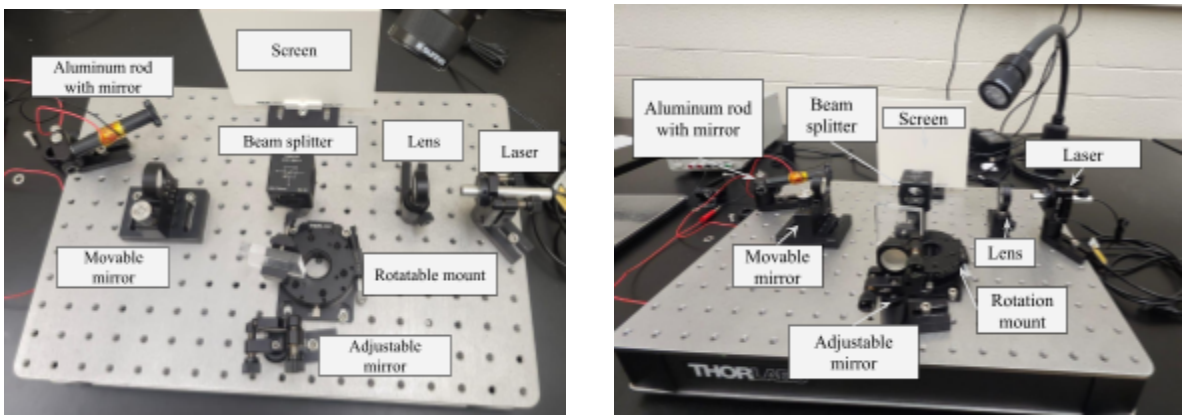

Figure 1: The setup for the Michelson Interferometer, from the top view (left) and the frontal view (right), with labels.

The interferometer was set up as in Figure 1, where the distance from the movable mirror to the beam splitter was within 0.01 mm of the distance between the beam splitter and the adjustable mirror, using a digital calliper. Once interference patterns were visible, the number of fringes that appeared or disappeared was counted while rotating the knob on the movable mirror. One scale division corresponds to the mirror moving one micrometre. The data were plotted as a linear function, with the slope corresponding to the laser wavelength, determined by Equation (1).

The index of refraction of a block was found by first placing a plastic square with a measured thickness in the holder of the rotation mount. The reference angle, where the beam was perpendicular to the square, was noted, and the mount was rotated at small angles, while the number of fringes was counted. The index of refraction was calculated by fitting data to Equation (2) and solving for n.

To measure the thermal expansion of aluminum, the movable mirror was replaced with an aluminum rod, and the mirror was realigned with the lens. The digital thermometer was used to record the base temperature, or the zero point (ZPD). The power source was turned on, and the voltage was increased in small increments. The temperature change was recorded after counting between 10 to 30 fringes reliably. Equation (3) was used to find the coefficient of thermal expansion, α, using the wavelength found for the green laser. At the start of each round, a new zero-point length and temperature were calculated, and the voltage was reset to 1V.

3. Data and Analysis

3.1 Wavelength of the Green Laser

Figure 2 below shows the number of fringes counted at various micrometre distances, along with their calculated wavelengths in nm using Equation (1).

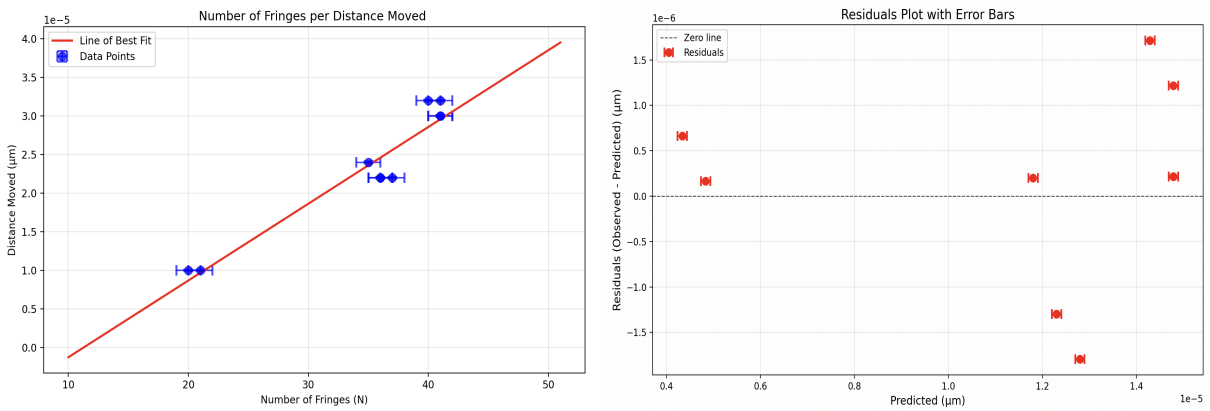

Figure 2: linear fit (right) and residual plot (left) of the number of fringes counted per distance moved according to Equation (1). The equation of the line is λ = (497±5)N +(-6±2) nm. The mean residual was 0 μm with a standard deviation of 0.5 μm. Vertical error bars in the linear fit and both error bars in the residuals plot are too small to be seen. Three data points overlap at N=41, and two overlap at N=36.

The linear fit yielded a chi-squared value of 1160 and a reduced chi-squared of 145. This high value means the data is vastly more scattered than the uncertainty estimates suggest. This may mean the assigned uncertainty (ΔN=±1) is too small to explain the scatter, indicating significant unaccounted-for systematic errors.

The slope, indicating the wavelength of the laser, is (497 ± *5 nm)*. From the residual plot, missing fringes can be seen at a distance between 2.5-3.0 μm, as the observed data points deviate substantially from the predicted path length. At 2.5 μm, the observed path length difference is lower than predicted, suggesting a smaller N value than expected was counted, meaning a fringe was missed. The cases where the observed values are higher than the predicted values mean that some fringes may have been counted twice, as the fringes are close to each other and could experience detection errors by the human eye.

The formula for error propagation is given in Equation (4).

$$\Delta\lambda = \lambda\sqrt{\frac{\Delta(2\Delta x)}{2\Delta x} + \frac{\Delta N}{N}} \tag{4}$$

The errors for the fringe count, ΔN, were taken as 1, by taking the standard deviation of the residuals (0.5 μm, in Figure (2)), and converting to N through Equation (1). The error in the movable mirror $\Delta(2\Delta x)$ was 0.1 degrees, based on the equipment showing up to the tenth decimal.

3.2. Index of Refraction of the Block

For a block (7.70 ± 0.01) mm thick, the data for the fringes are shown in Table (1), which are plotted with their fit in Figure (3). Small angles were taken with respect to a reference angle, where perturbing the rotatable mount would cause fringes to go from inward to outward. The wavelength was taken to be 497nm.

Counted fringes appearing (N) ± 1	14	19	56	21	56	9	25	16	14	4	22

Small angle of rotation (degrees, Θ) ± 0.1	3.0	-3.5	6	-3.5	6	-2.5	4	-3.0	3.0	-2.0	3.5

Table 1: The fringes counted to appear and disappear (N) while moving the rotating mount by small angles compared to the reference (Θ, in degrees).

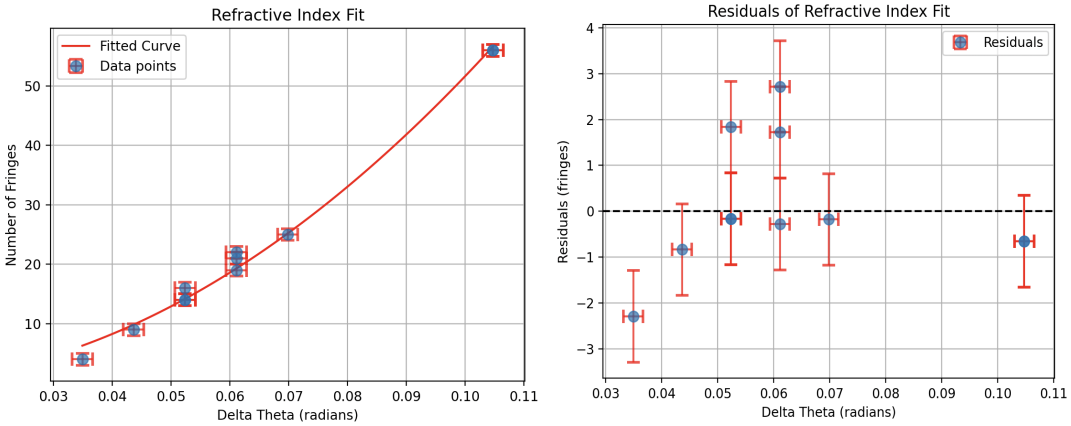

Figure 3: Fitted quadratic function of Equation (2) with n=1.50±0.01 (left), along with its residuals (right). The mean residual was 0.10, with a standard deviation of 1.37.

After converting the degrees to radians, and using Python to fit Equation (2) to the data in Table (1), we achieved an index of refraction of 1.50±0.01. The chi-squared value for this was 2.11, with a reduced chi-squared of 0.211. This value is smaller than 1, suggesting that the error bars (N ± 1 fringe) might be overestimated, and that there is overfitting.

The error was derived from the covariance, as provided by the SciPy fit in the code appendix. The formula used is explicitly shown in Equation (5), where Δn is the error and $pcov[0,0]$ is the covariance vector at index (0,0). The zeroth index is taken because we are only fitting for n [2].

$$\Delta n = \sqrt{pcov[0,0]} \tag{5}$$

More specifically, the covariance vector is given by Equation (9), for $N_f(i)$ the number of fringes counted for data point i, $f(\Theta_i; n)$ the expected value of Equation (2) given n (index of refraction) and Θ_i (small angle movement for datapoint i) , t the thickness of the block, and λ_g the wavelength of green light. We perform N-1 because we are only fitting one datapoint (n).

$$\Delta n = \sqrt{\frac{\sum_i [N_f(i) - f(\Theta_i; n)]^2}{(N-1)\left(\frac{t}{\lambda_g n^2}\right)^2 \sum_i (\Theta_i)^4}} \tag{6}$$

3.3. Thermal expansion of Al

The fringe counts for each temperature change, alongside initial and final lengths, are recorded in Table (2). These measurements are recorded with their fit in Figure (4).

Fringe count (N)	30	30	30	15	27
ΔT (ºC)	4.0	4.0	3.9	2.0	3.6
Initial Length L_0 (mm)	80.69	80.76	81.18	80.03	80.49
Final Length L (mm)	80.99	80.82	82.54	81.22	80.75

Table 2: Recorded values for fringe count (N), change in temperature (ºC), and initial and final lengths (mm) for the Aluminum rod under the green laser.

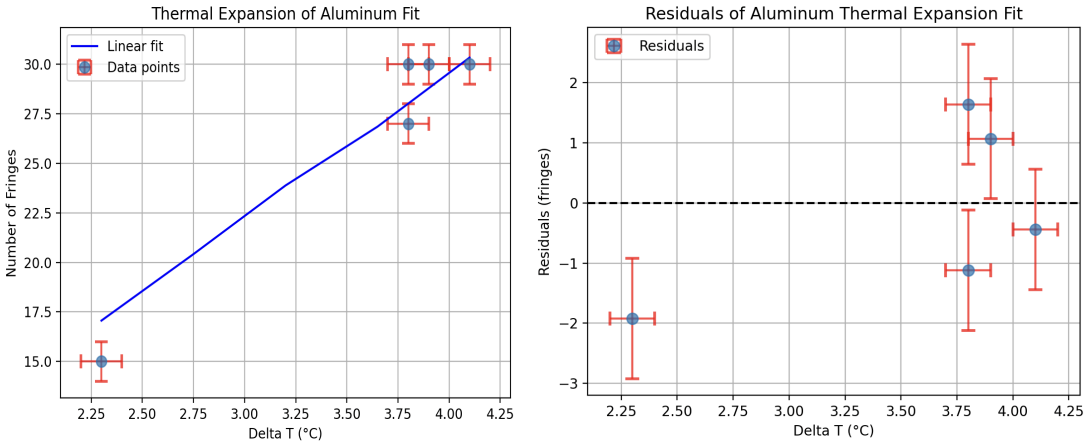

Figure 4: Fitted linear approximation of Equation (3) with α=2.28 x 10-5 1/K ±3.21 x 10^{-13} (left), along with its residuals (right). The mean residual was -0.15, with a standard deviation of 1.33.

The chi-squared value for the fit was 0.43, yielding a reduced chi-squared of 0.11. Similar to the index of refraction, this is also a small chi-squared value (less than 1, suggesting that the error bars might be overestimated, and that there is overfitting

After fitting the function in Python, a thermal expansion of around 2.28 x 10^{-5} 1/K was measured, with a covariance error of 3.21 x 10^{-13}. The error was derived from the covariance, as provided by the SciPy fit in the code appendix. Following Equations (5–6), the error for α, Δα, is given in Equation (7) [2].

$$\Delta\alpha = \sqrt{pcov[0,0]} \tag{7}$$

Equation (8) provides the entire formula for the error in α, for $N_f(i)$ the counted fringes for data point i, $f(\Delta T_i; \alpha)$ provided in Equation (3) for change in temperature ΔT_i for data point i, N the total number of datapoints, L_0 the initial length of the aluminum, and λ_g the wavelength of green light.

$$\Delta\alpha = \sqrt{\frac{\sum_i [N_f(i) - f(\Delta T_i;\alpha)]^2}{(N-1)\left(\frac{2L_0}{\lambda_g}\right)^2 \sum_i (\Delta T_i)^4}} \tag{8}$$

4. Discussion and Conclusion

The experiment successfully demonstrated the principles of wavelengths, index of refraction, and thermal expansion. The green laser had an experimental wavelength of (497±5) nm. This value has a percent difference of 0.6% with the lower bound of the typical range of green light, being 500nm [3]. The high reduced chi-squared value of 145 indicates poor fit with the data. This can stem from unquantifiable sources of errors, such as variation in the movement of the screw, or human errors in counting the number of fringes. This means statistical uncertainties from the resolution inadequately explained the data-model discrepancy and presented dominant systematic errors. A possible systematic error includes the shifting of fringes throughout the trials. If the movable mirror was accidentally tilted forward while conducting the trials, it could have led to the fringes shifting, making it possible to count more or less than intended. Additionally, even touching the movable screw without physically rotating it caused movements in the fringes. It is likely to have an error between when the counting of fringes was stopped and when the screw angle was measured, as even small angles produced fringes. Furthermore, there was evidence that fringe counts were missed from large variations in the residual plots, which is why the maximum fringe error of ±1 was taken. A source of error from the equipment can be due to not having the optimal contrast and resolution in the Michelson interferometer, which can lead to a mixing of colours and fringes, making fringes indistinguishable from others. It is also required that the mirrors are perfectly perpendicular to each other to get a perfectly zero path difference and the best resolution for detecting fringes, which is difficult to implement with human accuracy. While there are commonly polarization errors in a Michelson interferometer, due to modification of the light's polarization within the interferometer, it is unknown how significant this error is in limiting the intensity of the fringes.

The index of refraction was 1.50±0.01. It had a low reduced chi-squared value of around 0.211, suggesting overfitting. Assuming the block was glass, its index of refraction would be 1.5168 [4], leading to a percent difference of 1.035%. This shows that the experimental value aligns with the theoretical value. However, if the block is another material, then this value would have to be re-evaluated. A source of error could be that measuring the index of refraction assumes that the first medium through which the light travels is a vacuum. This is not accurate to reality, as there can be large pressure, temperature or humidity variations, creating differences between the two indices. This can cause discrepancies between the measured values, as they mimic different lab conditions, which are not standardized. Additionally, there can be errors in the gradual increase of the angles, as it may not be completely stable, causing fluctuations in comparison to the recorded value from the protractor [5]. Plotting the absolute value of the angle of rotation with the number of fringes calculated from Table (1) shows that the correlation between the angle of rotation and the number of fringes calculated is not completely linear for the small angles.

The coefficient of thermal expansion of Al was ($2.28 \times 10^{-5} \pm 3.21 \times 10^{-13}$) 1/K. It had a low reduced chi-squared value of around 0.11, suggesting overfitting. The value also differs by around 1.72% from the reported 23×10^{-6} 1/K [6], showing strong agreement. However, the extremely small covariance-derived error is likely an artifact of the fitting process and does not reflect the true experimental uncertainty, which is dominated by systematic errors. The most obvious error can be that there can be temperature fluctuations between when the trial ended to when the temperature was recorded. This would lead to a lower temperature reading than anticipated. To minimize this error, the thermometer was kept on the aluminum rod at all times to

get the most accurate possible reading. Moreover, it was noted that applying a slight pressure on the aluminum rod by touching it with the thermometer caused the fringe locations to deviate a little, making it slightly harder to track every streak. This was a trade-off to ensure the most accurate temperature. Additionally, there is high uncertainty in length measurement and noting the length change precisely using a calliper, where the extension is not quite large. Many experiments measuring the thermal expansion of aluminum instead incorporate vibration isolators and high-precision railing to be more precise in measuring [7,8]. Lastly, while going from one trial to another, a systematic error is that we created a new zero-point length and temperature for each trial. As both temperature and length can fluctuate with time, there can be a delay between when the zero-temperature was recorded and the experiment was started, or the aluminum rod could be actively contracting to its regular length when there is only a minimum amount of voltage applied, before being forced to extend once the aluminum gets warmer again.

In conclusion, the experiment validated Equations (1), (2), and (3), within 2% difference (in total) of reported experimental values of green light, index of refraction of glass, and the thermal expansion coefficient of aluminum. It highlighted that while our values were very similar to literature values, systematic errors could cause high uncertainties and a reduced chi-squared value. Therefore, it may not be possible to produce the same results in all circumstances and still yield similar results. This attributes to limitations like fluctuating temperatures, vibrations leading to small movements of the fringes, and a suboptimal resolution, which can cause undistinguishable fringes. This process can be improved by finding ways to further increase the sizing of the fringes to they are much more visible, while ensuring they do not deviate due to small external forces and vibrations.

5. Appendix

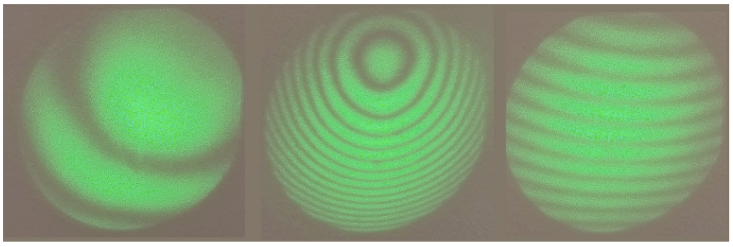

Figure 1: A schematic diagram of the Michelson interferometer. Left: the path lengths are nearly identical, and the alignment is almost centred. Middle: the path lengths differ by hundreds of wavelengths, but the alignment is almost centred. Right: the alignment is off (the center is above the image).

Figure 1: excerpt from the Lab document [1], showing what ideal interference patterns should look like.

6. References

[1] J. Vise, C. Lee, B. Wilson, P. Albanelli, and S. Fomichev, “Interferometry,” July 2025. Available: https://www.physics.utoronto.ca/~phy224_324/LabManuals/Interferometers.pdf. [Accessed: Oct. 26, 2025]

[2] “Covariance — SciPy V1.16.2 Manual.” Scipy.org, 2025, docs.scipy.org/doc/scipy/reference/generated/scipy.stats.Covariance.html. Accessed 9 Nov. 2025.
[3] Runkle, Erik. “Growing Plants with Green Light.” GPNMAG.COM, Michigan State University. Accessed 8 Nov. 2025.
[4] M. N. Polyanskiy, “Refractiveindex.info database of optical constants,” vol. 11, no. 1, p. 94, Jan. 2024, doi: 10.1038/s41597-023-02898-2. Available: https://www.nature.com/articles/s41597-023-02898-2. [Accessed: Nov. 08, 2025]
[5] Fendley, J J. “Measurement of Refractive Index Using a Michelson Interferometer.” *Physics Education*, vol. 17, no. 5, 1 Sept. 1982, pp. 209–211, https://doi.org/10.1088/0031-9120/17/5/001.
[6] “Thermal Expansion”, Available: https://www.aplusphysics.com/courses/honors/thermo/expansion.html. [Accessed: Nov. 08, 2025]
[7] Luo, Weipeng, et al. “Robust Interferometry for Testing Thermal Expansion of Dual-Material Lattices.” *Materials*, vol. 13, no. 2, 9 Jan. 2020, p. 313, https://doi.org/10.3390/ma13020313. Accessed 14 May 2023.
[8] Ducourtieux, Sébastien. *Toward High Precision Position Control Using Laser Interferometry: Main Sources of Error*. 2018.